3D Posture Visualisation From Body Shape Measurements Using Physics Simulation, to Ascertain the Orientation of the Pelvis and Femurs in a Seated Position

Adam Partlow , Colin Gibson , Janusz Kulon

PII: S0169-2607(20)31605-9
DOI: https://doi.org/10.1016/j.cmpb.2020.105772
Reference: COMM 105772

To appear in: *Computer Methods and Programs in Biomedicine*

Received date: 2 June 2020
Accepted date: 19 September 2020

Please cite this article as: Adam Partlow , Colin Gibson , Janusz Kulon , 3D Posture Visualisation From Body Shape Measurements Using Physics Simulation, to Ascertain the Orientation of the Pelvis and Femurs in a Seated Position, *Computer Methods and Programs in Biomedicine* (2020), doi: https://doi.org/10.1016/j.cmpb.2020.105772

Highlights

- Novel physics simulation can visualise the pelvis and femurs in a seated posture.
- Simulation is an alternative to machine learning when datasets are small.
- Visualisation makes it easier to communicate posture for clinical purposes.
- Body shape measurements enable the comparison of seated posture over time.
- Comparison of posture over time can be used as an outcome measure.

3D Posture Visualisation From Body Shape Measurements Using Physics Simulation, to Ascertain the Orientation of the Pelvis and Femurs in a Seated Position

Adam Partlow[a] adam.partlow@wales.nhs.uk, corresponding author.

Colin Gibson[a] colin.gibson@wales.nhs.uk

Janusz Kulon[b] j.kulon@southwales.ac.uk

[a] Rehabilitation Engineering Unit, Artificial Limb & Appliance Service, Cardiff & Vale University Health Board, CF37 5TF, UK

[b] Faculty of Computing, Engineering and Science, University of South Wales, Pontypridd, CF37 1DL, UK

Abstract

Background and Objective: The paper presents a novel technique for the visualisation and measurement of anthropometric features from patients with severe musculoskeletal conditions. During a routine postural assessment, healthcare professionals use anthropometric measurements to infer internal musculoskeletal configuration and inform the prescription of Custom Contoured Seating systems tailored to individual needs. Current assessment procedures are not only time consuming but also do not readily facilitate the communication of musculoskeletal configuration between healthcare professionals nor the quantitative comparison of changes over time. There are many techniques measuring musculoskeletal configurations such as MRI, CT or X-ray. However, most are very resource intensive and do not readily lend themselves to widespread use in, for example, community based services. Due to the low volume of patient data and hence small datasets *modern* machine learning techniques are also not feasible and a bespoke solution is required.

Methods: The technique outlined in this paper uses physics simulation to visualise the orientation of the pelvis and femurs when seated in a custom contoured cushion. The input to the algorithm is a body shape measurement and the output is a visualised pelvis and femurs. The algorithm was tested by also outputting a multi-label classification of posture (specific to the pelvis and femurs).

Results: The physics simulation has a classification accuracy of 72.9% when labelling all 9 features of the model; when considering 6 features (excluding rotations about the x-axis) the accuracy is increased to 92.8%.

Conclusions: This study has shown that a mechanical shape sensor can be used to capture the unsupported seated posture of an individual during a clinic. The results have demonstrated the potential of the physics simulation to be used for anthropometric feature extraction from body shape measurements leading to a better posture visualization. Capturing and visualising the seated posture in this way should enable clinicians to more easily compare the effects of clinical interventions over time and document postural changes. Overall, the algorithm performed well, however, in order to fully evaluate its clinical benefit, it needs to be tested in the future using data from patients with severe musculoskeletal conditions and complex body shapes.

Keywords

Visualization, Medical simulation, Physics computing, Engineering in medicine and biology, Biomedical engineering, Biomedical informatics.

1 Introduction

Clinical engineers creating custom contoured seats have to infer a patient's internal skeletal configuration by palpating skeletal landmarks during assessments and reviewing recorded clinical data when the patient is not present. The internal skeletal configuration and the changes in a patient's posture between two points in time before and after a clinical intervention are important factors when deciding what posture a patient should be supported in whilst seated in their custom contoured seat. This can often be difficult to visualise. When supporting and correcting a patient's posture with a custom contoured seat clinical engineers must ensure that they are not affecting the patient adversely by over-correcting or failing to notice a condition which is then left unmanaged.

Changes in posture over time due to neuro-musculoskeletal conditions are difficult to describe in detail even with the succinct vocabulary used by clinicians. For this reason, whilst designing the patient's custom contoured seating clinical engineers spend extended periods of time assessing the musculoskeletal capabilities of a patient and communicating with other experts that deliver the patient's care. Communicating complex musculoskeletal conditions, postural capabilities and changes to conditions and capabilities over-time to other experts and professionals is not trivial.

There are various techniques that can be used to communicate posture, capture the position of anthropometric landmarks and measure the severity of musculoskeletal conditions. Internal anthropometric landmarks can be located using imaging techniques such as X-ray, MRI or CT. These techniques allow clinicians to accurately pinpoint the location of specific spinal and pelvic landmarks and record their positions; informing posture. Calculations such as the Cobb angle for spinal curvature and acetabular index for hip dislocation, for example can be performed on internal anthropometric landmarks. These measurements can be used to inform clinicians as to the severity of musculoskeletal conditions which are then used to record and communicate these to other professionals.

External measurement tools such as Moiré photography, contour devices and inclinometers can be used to capture the shape of a patient's back and the angle of flexion of the hips while seated. These tools are not used to provide accurate measurement of the position and angles of an internal landmark but a ‘fuzzy’ qualitative measure of a condition. These measurements are then used to inform discussions of the postural condition and communicate its severity to other clinicians.

Postural assessments which rely on measurement and palpating external bony landmarks are used to describe the sitting ability of a patient. Aissaoui et al. [1] used an articulated mechanical arm to digitize external pelvic landmarks. The absolute accuracy of the coordinate localisation was 0.64 mm, however for each posture, the subjects were required to sit still for at least 4 min, then, the digitization of the anatomical and simulator chair markers were collected. Posturography tests [2] and trunk support systems [3] have been used in laboratory and clinical settings to assess postural control in individuals lacking independent sitting. Tools such as the gross motor function classification system (GMFCS) [4] or the neutral-zero method [5, 6] involve making observations of

the patient and scoring their ability on a worksheet. These tools generally take a significant amount of time to use but provide a thorough assessment of sitting ability.

Problems exist with current processes. The imaging techniques are time consuming and expensive and it is not practicable to perform these at every postural assessment. Secondly, the imaging techniques and the external measurement techniques require a patient to stand or lay down. It is often not possible for patients to stand and the measurement is not performed in a seated posture so it has limited application to the design of custom contoured seating [7]. The majority of external measurements of the back and lower extremities are not captured simultaneously and so the patient may be moved while the measurements are being taken. A technique that captures the back and lower extremities simultaneously while in a seated posture would be ideal for measuring a patient's posture over time to determine clinical outcomes of seating interventions.

The aforementioned techniques that have been outlined for capturing and communicating posture are inappropriate for use on the group of patients that require custom contoured seating at Cardiff and Vale University Health Board's (UHB) Rehabilitation Engineering Unit (REU). A study is currently ongoing at Cardiff and Vale UHB REU to create a customisable digital human model (DHM) and to investigate the feasibility of using current clinical practices to configure the DHM [8, 9].

DHMs can be used to represent an individual or group of individuals in computer simulations and then design ergonomic solutions that are tailored to the individual's needs. They can be used to represent a patient's internal skeletal configuration, simulate the effect of an intervention, or improve communication between professionals [10]. When using a DHM it must be configured so that it represents the current patient that the clinician is treating. To configure DHMs users can input values, for example: joint angles, joint ranges of motion (ROM), scale of the DHM and positions of specific anatomical landmarks. Some applications do not use a specialised DHM tailored to the patient and instead can use a p-th percentile model that represents p of the population. The input values to manipulate a DHM must either be manually entered by the user or generated by another device that can then automatically position the DHM.

For a DHM to be used effectively in a special seating environment the DHM must be configured to represent the patient's posture at the time of assessment. There are many techniques which exist for extracting the position of external anthropometric landmarks to configure DHMs. Popular techniques for configuring DHMs include motion capture as used in gait analysis [11, 12], stereo photography [13, 14] and input from imaging techniques such as X-ray and magnetic resonance imaging (MRI) [10], [13, 15]. Currently, these techniques have not been demonstrated to be suitable for capturing a static seated posture at a discrete moment in time. X-ray and MRI are not suitable for capturing the seated posture of an individual whilst seated in a wheelchair due to the wheelchair's materials interfering with the measurement or being unsafe. Stereo photography and gait analysis require visual line of sight to the landmarks being measured and hence it is difficult to capture the seated posture of an individual. In such postural assessments the landmarks are often obstructed by the presence of a clinician or the surface of the seat. More recently, developments are being made using small non-invasive devices such as ultrasonic transducers (employing indoor acoustic localisation) and CMM (coordinate measuring machine) arms to take measurements of a patient's external anthropometric landmarks in order to define the posture of a patient [16, 17, 18].

As stated previously, imaging techniques are inappropriate for the Cardiff and Vale UHB REU patient group. They are often unable to stand or sit unsupported during the imaging process and repeatedly imaging this patient group would be resource intensive. A specialised DHM for use on the patients of Cardiff and Vale UHBs REU is being developed. Cardiff and Vale UHB REU use a device named the Cardiff Body Match (CBM) (Figure 1) to capture the seated shape of a patient's body [7, 19]. The shape is used to create a custom contoured seat that conforms to the contours of the patient's body and distributes pressure evenly across the surface. This provides postural support whilst minimising the risk of pressure related injuries. The shape data captured by the CBM contains surface contours of a patient's posterior aspects of the thighs, buttocks and trunk.

The problems that have been outlined in this section include the difficulty in recording posture clearly and reliably; and communicating posture to other professionals succinctly. The work presented in this study aims to visualise the position of an individual's pelvis and femurs using non-invasive techniques whilst in a seated posture. This would allow quantitative recording of people's posture and allow the comparison of posture over time for the measurement of clinical outcomes. Whilst this study has initially focussed on the application to custom contoured seating users; the techniques described in this article are applicable to any body shape measurement of the pelvis and femurs in a seated position.

This article presents the work completed to date in order to identify the position and orientation of the pelvis and femurs in a CBM measurement for input into a DHM and visualisation of the seated posture. The calculated skeletal landmarks can then be used to inform a DHM as to the location of certain anthropometric features to position the model, or used to calculate clinical measurements which are used to analyse posture to determine sitting capabilities.

Figure 1: The CBM mechanical shape sensor.

2 Method

The algorithm described in this article uses physics simulation to estimate the position of the pelvis and femurs in a seated posture. The input into the algorithm is a body shape measurement of the anterior aspect of the patient's trunk; abdomen and lower limbs in a seated posture. The output of the technique is a visualised pelvis and femurs and, for testing purposes a multi-label classification of the orientation of the pelvis and femurs.

The input measurements are captured using a device named the Cardiff Body Match (CBM) (Figure 1) which is a mechanical shape sensor used clinically to create custom contoured seating systems in Cardiff and Vale University Health Board's (UHB) Rehabilitation Engineering Unit (REU) [7].

The classification of the orientation of the pelvis and femurs is obtained by first *dropping* an anatomically correct mesh of the pelvis and femurs onto the input body shape measurement and allowing the mesh to come to rest. The rotations of the pelvis relative to a neutral pelvis and femurs relative to the pelvis are then used to calculate the classification.

Physics simulations rely on the correct material properties and parameters being defined in order for them to produce *realistic* movements. This study also attempts to identify the optimum parameters for the simulation by searching a range of values and assessing the accuracy of the algorithm when using each set of parameters.

The following sections outline how the algorithm is developed and tested.

2.1 Simulation Input Data

The input into the physics simulation is a body shape measurement. Body shape measurements at Cardiff and Vale UHBs REU are captured using the CBM mechanical shape sensor pictured in Figure 1 The CBM was developed at Cardiff and Vale UHBs REU [7] and measures the contours of an individual's body in a seated position. In this study only the measurement from the base cushion (Figure 2a) is used as the simulation is not taking into account the trunk. The sitting surface is composed of a ROHO Quadtro Select High Profile cushion [20] without its cover and the backrest of the CBM is a grid of pins which are displaced by, and remain in contact with the patient’s body, and hence measures body shape.

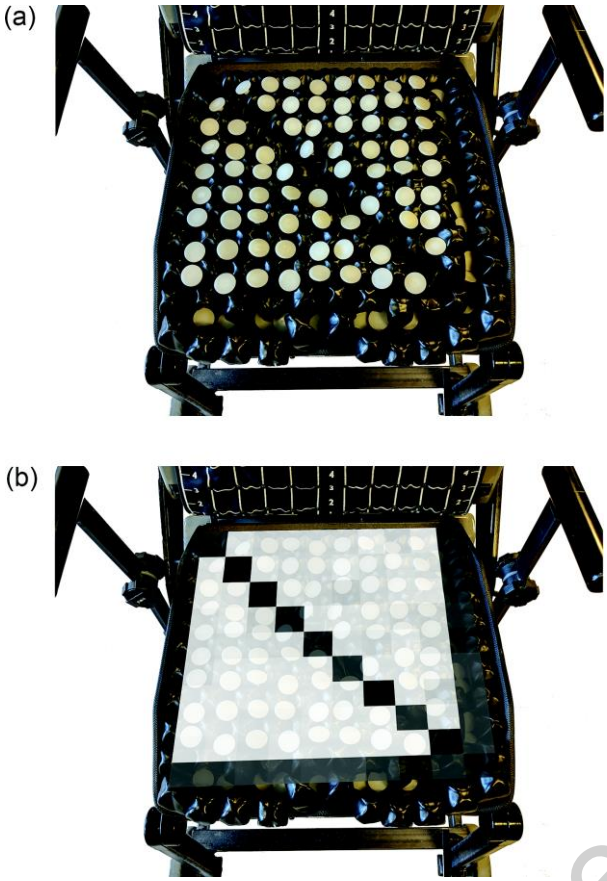

(a) CBM base cushion with some pins depressed (b) Cushion with measurement superimposed

Figure 2: CBM shape sensor after a measurement is taken and the measurement superimposed on the CBM shape sensor.

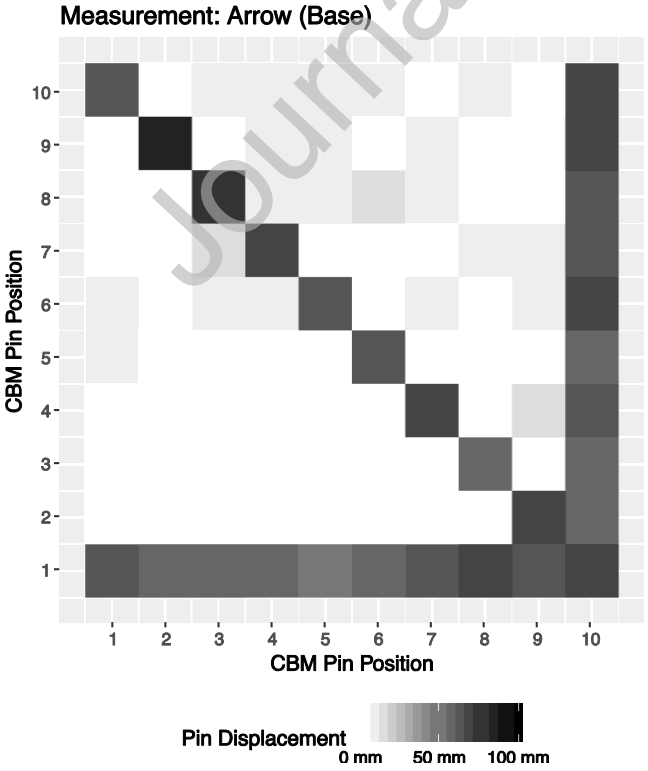

Figure 3: A CBM measurement visualised as a height map.

In order to create a CBM measurement, a patient is seated on the CBM with the cushion inflated, all base pins extended and all back pins retracted. The air is then released from the cushion to stabilise the pelvis, as the pelvis sinks into the cushion the base pins are displaced. When the pelvis is stable the clinicians will position the patient's trunk in a position that is deemed optimum for them, the back pins are then extended and they stop when they come into contact with the patient or are fully extended. At this point the displacement of all the pins are captured which are then recorded as CBM base and back measurements. CBM measurements can be used to create a pressure relieving posture supporting cushion. By virtue of the CBMs design [8, 19] pressure is automatically evenly distributed. The final shape of the cushion is determined by the patient's posture and hence the shape of the CBM measurement. Figure 2a shows an image of the CBM base after a measurement has been taken. This measurement is visualised in Figure 3. The CBM measurement in Figure 3 is shown superimposed onto the CBM base in Figure 2b.

A CBM measurement consists of a 10×10 matrix, $\boldsymbol{M}$ whose elements are the displacement values of the CBMs pins. CBM measurements are measured in millimetres and are stored as a vector of values, $\boldsymbol{p}$. The order of the elements in the vector is given by (1)-(4).

$$p = \begin{bmatrix} p_1 \\ p_2 \\ \vdots \\ p_i \\ \vdots \\ p_n \end{bmatrix} : i = \mathbb{N} \in \{1, \dots, p_n\} \quad (1)$$

$$p_i \coloneqq \boldsymbol{M}_{rc} \quad (2)$$

$$c \coloneqq c_n - \big((i-1)\ mod\ c_n\big) \quad (3)$$

$$r \coloneqq \left\lceil \frac{i}{r_n} \right\rceil \quad (4)$$

Where $\boldsymbol{M}_{rc}$ is an element in the matrix $\boldsymbol{M}$, r and c are the current row and column number in the matrix $\boldsymbol{M}$ respectively given the i-th element in the vector $\boldsymbol{p}$. r_n and c_n are the total number of rows and columns in the measurement. In an unmodified CBM measurement straight from the CBM shape sensor $r_n = c_n = 10$ and $r_n c_n = p_n = 100$. A CBM measurement matrix $\boldsymbol{M}$ can be visualised as a height map as shown in Figure 3. In order to use the CBM measurement in the physics simulation a triangle mesh must be created.

2.2 Physics Simulation

Previous studies have reviewed the accuracy and repeatability of several open source and freely accessible physics libraries and stated that the Bullet physics library [21] should be used for accurate simulation [22, 23]. The Bullet physics library is a deterministic system and will always produce the same results given the same starting conditions. The physics simulation was scripted in Python and visualised using Blender [24].

The Bullet physics library states that dimensions should be in metres and when the simulation involves objects which are less than 20 cm in any dimension the time step, Δt of the simulation

should be adjusted. It is suggested in the Bullet physics user guide [25] that $\Delta t = 1/300$ sec be used for objects as small as a 1 cm die. In this simulation some of the bony prominences of the pelvis and femurs are small and for this reason the recommended time step is used, $\Delta t = 1/300$ sec, i.e. 300 simulation steps per second.

Coefficient	Symbol	Value(s) Tested
Friction of cushion	μ_c	$\{0.00, 0.10, \dots, 1.00\}$
Restitution of cushion	e_c	$\{0.00, 0.10, \dots, 1.00\}$
Mass of cushion	m_c	∞
Friction of skeleton	μ_s	1.00
Restitution of skeleton	e_s	1.00
Mass of pelvis	m_p	4.780 kg
Mass of femur	m_f	1.705 kg
Starting x-coordinate	x	$\{-0.2, -0.16, \dots, 0.2\}$ m
Starting y-coordinate	y	$\{-0.2, -0.16, \dots, 0.2\}$ m
Starting z-coordinate	z	0.3 m

Table 1: Summary of parameters used in the physics simulation, their symbols and values.

The physics simulation used a 50th percentile human male pelvis and femurs [26] to estimate the sitting position of the patient. This is appropriate for this study as the participants are both male but future work will need to take into account the differences between male and female musculoskeletal structures and mechanics. The pelvis and femurs are *dropped* onto the seating surface where they eventually come to rest. The resting position was determined by the parameters used in the physics calculations, the parameters have been summarised in table 1. The coefficients of friction μ and restitution e need only be changed for one rigid body as the calculation for friction and restitution within the Bullet physics engine is multiplicative. The coefficients of the cushion are adjusted whilst other rigid bodies' coefficients remain at a value of 1. Empirical testing demonstrated that a maximum value for e_c should be 1.4; values higher than this cause the skeletal mesh to be thrown from the cushion due to the high value of the elastic coefficient.

2.2.1 Seating Surface

The triangle mesh for the physics simulation is calculated from the CBM pin measurement vector, $\boldsymbol{p}$. (5)-(9) generates the vertex coordinate matrix, $\boldsymbol{V}$ for a triangle mesh that represents the seating surface. Where the coefficient 0.04445 is the resolution of the CBM mechanical shape sensors in millimetres (1.75'').

$$V = \begin{bmatrix} v_1 \\ v_2 \\ \vdots \\ v_i \\ \vdots \\ v_n \end{bmatrix} : i = \mathbb{N} \in \{1, \dots, v_n\} \quad (5)$$

$$v_i \coloneqq [0.04445c, -p_j, 0.04445r] \quad (6)$$

$$c \coloneqq (i-1) - (rr_n) \quad (7)$$

$$r \coloneqq \left\lfloor \frac{i-1}{r_n} \right\rfloor \quad (8)$$

$$j \coloneqq rr_n + c + 1 \quad (9)$$

Where v_i is the i-th row of the vertex matrix $\boldsymbol{V}$, and c and r are the current row and column of the CBM measurement matrix. j, defined in (9) is the j-th element of $\boldsymbol{p}$ containing the CBM pin measurement used to assign the y-coordinate of the current vertex. The triangle mesh's indices, $\boldsymbol{T}$, are calculated using (10)-(14).

$$T = \begin{bmatrix} t_1 \\ t_2 \\ \vdots \\ t_i \\ \vdots \\ t_n \end{bmatrix} \quad (10)$$

$$n \coloneqq 2(r_n - 1)(c_n - 1) \quad (11)$$

$$t_i \coloneqq \begin{cases} f_1 \text{ for } i \leq \frac{t_n}{2} \\ f_2 \text{ for } i > \frac{t_n}{2} \end{cases} \quad (12)$$

$$f_1 = \begin{bmatrix} i + \left\lfloor \frac{i}{c_n} \right\rfloor \\ i + c_n + \left\lfloor \frac{i}{c_n} \right\rfloor \\ i + 1 + \left\lfloor \frac{i}{c_n} \right\rfloor \end{bmatrix} \quad (13)$$

$$f_2 = \begin{bmatrix} i - \frac{t_n}{2} + \left\lfloor \frac{\left(i - \frac{t_n}{2}\right)}{c_n} \right\rfloor + c_n \\ i + 1 - \frac{t_n}{2} + \left\lfloor \frac{\left(i - \frac{t_n}{2}\right)}{c_n} \right\rfloor + c_n \\ i + 1 - \frac{t_n}{2} + \left\lfloor \frac{\left(i - \frac{t_n}{2}\right)}{c_n} \right\rfloor \end{bmatrix} \quad (14)$$

Where t_i is the i-th row of the triangle mesh's index matrix and t_n is the total number of triangles in the mesh, calculated using (11).

The indices in $\boldsymbol{T}$ and the vertices in $\boldsymbol{V}$ are used by the Bullet physics library to create a kinematic object which does not move during a simulation. The kinematic object represents the seating surface

which is used to accommodate the pelvis and femurs of the skeletal model being positioned in the seat.

2.3 Skeletal Model

The Zygote human male skeletal model is used as the basis for the skeletal model in the simulation. The Zygote model `was developed from CT scans of a 50th percentile male, and was carefully modelled to retain subtle anatomical nuances unique to specific bones.' [26]

The study performed physics simulation on dynamic objects representing the pelvis and femurs which are concave shapes. The Bullet physics library does not have a collision solver that is able to calculate collisions between dynamic concave meshes directly. Therefore Bullet requires that collisions involving concave meshes are performed on decomposed meshes constructed with convex hulls. Bullet recommends using the V-HACD algorithm to perform mesh decomposition. The pelvis and femurs are not convex in shape and so are segmented into a series of convex hulls using the V-HACD algorithm [27].

Bone	Feature	Original	Decomposed
Pelvis	Vertices	358,047	558
Pelvis	Triangles	718,474	1,040
Left Femur	Vertices	33,515	256
Left Femur	Triangles	67,033	480
Right Femur	Vertices	33,546	224
Right Femur	Triangles	67,092	420

Table 2: Mesh complexity before and after decomposition using the V-HACD algorithm.

2.3.1 Bounding Volume

The decomposed bounding volumes created by the V-HACD algorithm [27] significantly reduce the complexity of the models whilst maintaining the detail. Table 2 summarises the changes in mesh complexity between the original skeletal meshes and the V-HACD output. Figure 4 shows the visual differences between the original mesh and the decomposed meshes.

2.3.2 Joint Constraints

The interactions between the cushion and skeletal meshes require that joint constraints between the pelvis and femurs are defined to enable `realistic' motion about the joints. The study by Ryf and Weymann [5, 6] investigated joint ranges of motion for a large population. This study forms the basis of techniques widely used by clinicians to measure joint ranges of motion and assess their function. Due to the neutral-zero methods wide usage and recognisability amongst professionals in postural management the ranges of motion quoted in these studies are used as the limits for the skeletal model. The ranges of motion for the hip joint are summarised in table 3 and visualised in Figure 5.

The reference posture in this study is standing upright. Standing upright would be recorded as 0° abduction/adduction, 0° flexion/extension and 0° internal/external rotation.

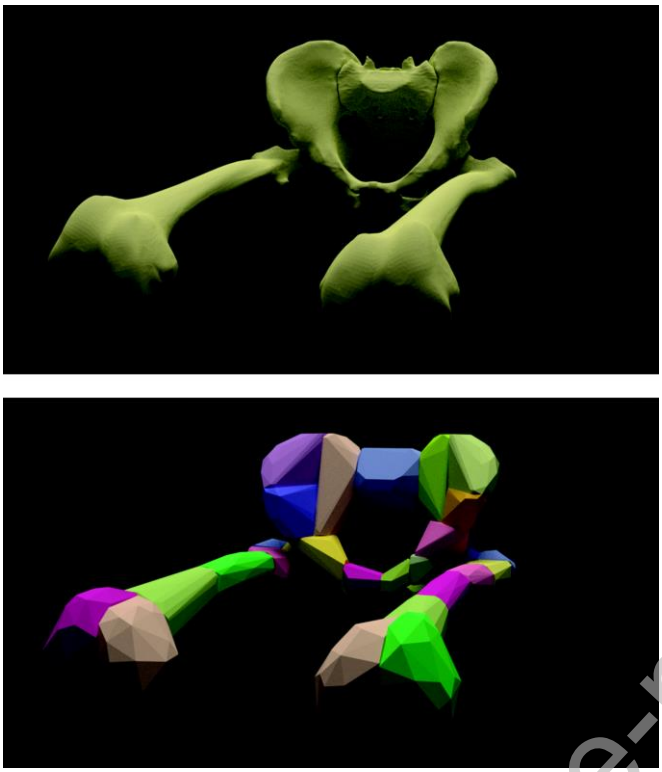

(a) Original mesh (b) Decomposed mesh

Figure 4: The original mesh of the pelvis and femurs and the decomposed mesh.

(a) Transverse plane, γ rotations. (b) Coronal plane, β rotations. (c) Sagittal plane, α rotations.

Figure 5: Descriptions for orientation of the pelvis and ranges of motion at the hip joint.

Rotation about the hip joint	neutral-zero measurement
Abduction / Adduction	50° - 0° - 20°
Flexion / Extension	130° - 0° - 10°
Internal / External Rotation	30° - 0° - 40°

Table 3: Ranges of motion used for the physics simulation. Reference posture is standing upright.

2.4 Test Data

To validate the output of the simulation, control data was collected from 2 able bodied healthy subjects in 7 different postures. The 7 different postures were: sitting normally; leaning to the right;

leaning to the left; pelvic obliquity down on the right; pelvic obliquity down on the left; pelvic tilt; and clutching the knees with a rounded back. Some of the postures were recorded more than once resulting in 23 postures overall. Each posture was measured independently of any previous measurements. The CBM shape sensor was reset after each measurement.

In addition to the CBM measurements that were captured, the rotation at the hips and pelvis were recorded by clinicians. The orientation of the femurs and the pelvis while seated in the CBM was used to validate the physics simulation output. Figure 6 shows an example of an ideal output of the simulation, in this instance the model has been positioned and oriented manually.

2.5 Output Data

The simulation outputs 9 measurements which are derived from the final resting position of the pelvis and femurs. These values are pelvic tilt, rotation, and obliquity and flexion/extension, adduction/abduction and internal/external rotation of the left and right hips. In order to compare these results to those which are collected during a clinical assessment the numerical values must be classified into one of three categories.

Figure 5 shows the classes that describe the orientation of the pelvis or femur based on the angle of rotation about an axes used during clinical assessments to record an individual's posture (they have not been created exclusively for this study). Where α, β and γ are the rotations about the x, y and z axes respectively as stated in Partlow [7].

Figure 6: Control Participant 1 seated in the pelvic obliquity posture (participant 1, measurement 6, obliquity 1), the participant is attempting to rotate their pelvis such that it is considered down on the left. Note however that it is difficult for an able-bodied person to achieve the level of rotation observed in those with musculoskeletal conditions. The right hip is flexed.

2.6 Testing

The algorithms prediction was compared to the test data and the accuracy for each set of input parameters as defined in Table 1 and for each of the 9 features measured by the simulation was calculated. The top 10 accuracies for each of the features will be examined and discussed.

3 Results

The physics simulation was run on each of the 23 measurements. The parameters used in the physics simulation are shown in Table 1. This resulted in 16,500 permutations per measurement resulting in 379,500 results. This section outlines how each set of parameters effected the classification performance of the algorithm. This was measured using the overall accuracy as defined in (15). Where n is the number of measurements; Y_i are the known labels of the observation

(determined by a clinician at the time of measurement); and Z_i are the predicted labels for the observation(determined by the output of the algorithm).

$$Accuracy \coloneqq \frac{1}{n}\sum_{i=1}^{n}\frac{|Y_i \cap Z_i|}{|Y_i \cup Z_i|} \qquad (15)$$

The greatest overall accuracy was 72.9%. This was obtained when the simulation parameters were $\mu_C = 1$, $e_c = 0$, and the starting location was $P_{(x,y,z)} = [0.02, 0.11, 0.3]$ metres. The 10 greatest accuracies are shown in Table 4.

		Initial Pelvis COM			Accuracy (%)									
μ_c	e_c	x	y	z	P_α	P_β	P_γ	L_α	L_β	L_γ	R_α	R_β	R_γ	Overall
1.0	0.0	0.02	0.11	0.3	13.0	82.6	100.0	69.6	87.0	87.0	60.9	87.0	69.6	72.9
1.0	0.0	-0.02	0.11	0.3	13.0	100.0	100.0	47.8	95.7	69.6	47.8	95.7	82.6	72.5
1.0	0.1	0.02	0.11	0.3	17.4	87.0	95.7	56.5	87.0	78.3	65.2	91.3	65.2	71.5
0.4	0.2	0.02	0.11	0.3	17.4	91.3	95.7	60.9	87.0	69.6	65.2	82.6	69.6	71.0
0.7	0.2	0.02	0.11	0.3	21.7	87.0	100.0	47.8	91.3	69.6	65.2	91.3	65.2	71.0
1.0	0.2	-0.02	0.11	0.3	13.0	91.3	100.0	56.5	95.7	56.5	60.9	95.7	65.2	70.5
0.9	0.4	0.02	0.11	0.3	13.0	100.0	95.7	65.2	91.3	56.5	60.9	87.0	65.2	70.5
1.0	0.1	-0.02	-0.02	0.3	73.9	95.7	100.0	52.2	100.0	39.1	52.2	78.3	39.1	70.0
0.7	0.0	-0.02	0.11	0.3	4.3	95.7	95.7	47.8	100.0	78.3	43.5	91.3	73.9	70.0
0.9	0.0	-0.02	0.11	0.3	8.7	100.0	100.0	30.4	95.7	73.9	34.8	100.0	87.0	70.0

Table 5: The 10 results with the highest overall accuracy; the per feature accuracies; and the parameters for the simulation.

		Initial Pelvis COM			Accuracy (%)						
μ_c	e_c	x	y	z	P_β	P_γ	L_β	L_γ	R_β	R_γ	Overall
1.0	0.0	0.02	0.11	0.3	82.6	100.0	87.0	87.0	87.0	69.6	72.9
1.0	0.0	-0.02	0.11	0.3	100.0	100.0	95.7	69.6	95.7	82.6	72.5
1.0	0.1	0.02	0.11	0.3	87.0	95.7	87.0	78.3	91.3	65.2	71.5
0.4	0.2	0.02	0.11	0.3	91.3	95.7	87.0	69.6	82.6	69.6	71.0
0.7	0.2	0.02	0.11	0.3	87.0	100.0	91.3	69.6	91.3	65.2	71.0
1.0	0.2	-0.02	0.11	0.3	91.3	100.0	95.7	56.5	95.7	65.2	70.5
0.9	0.4	0.02	0.11	0.3	100.0	95.7	91.3	56.5	87.0	65.2	70.5
1.0	0.1	-0.02	-0.02	0.3	95.7	100.0	100.0	39.1	78.3	39.1	70.0
0.7	0.0	-0.02	0.11	0.3	95.7	95.7	100.0	78.3	91.3	73.9	70.0
0.9	0.0	-0.02	0.11	0.3	100.0	100.0	95.7	73.9	100.0	87.0	70.0

Table 6: The 10 results with the highest overall accuracy excluding alpha rotations; the per feature accuracies; and the parameters for the simulation.

When excluding alpha rotations from the classification the highest overall accuracy was 92.8%. This was obtained when the simulation parameters were $\mu_c = 0.9$, $e_c = 0$, and the starting location was $P_{(x,y,z)} = [-0.02, 0.11, 0.3]$ metres. The 10 greatest accuracies are shown in Table 5. The overall accuracy for all permutations is shown in Figure 7.

Figure 8 shows the output visualised measurement for 4 of the 23 measurements overlaid on a photo of the assessment. During the assessments the position of the cameras were fixed. This allowed for the datum of the seating surface of the CBM shape sensor to be aligned with the datum of the seating surface in the simulation.

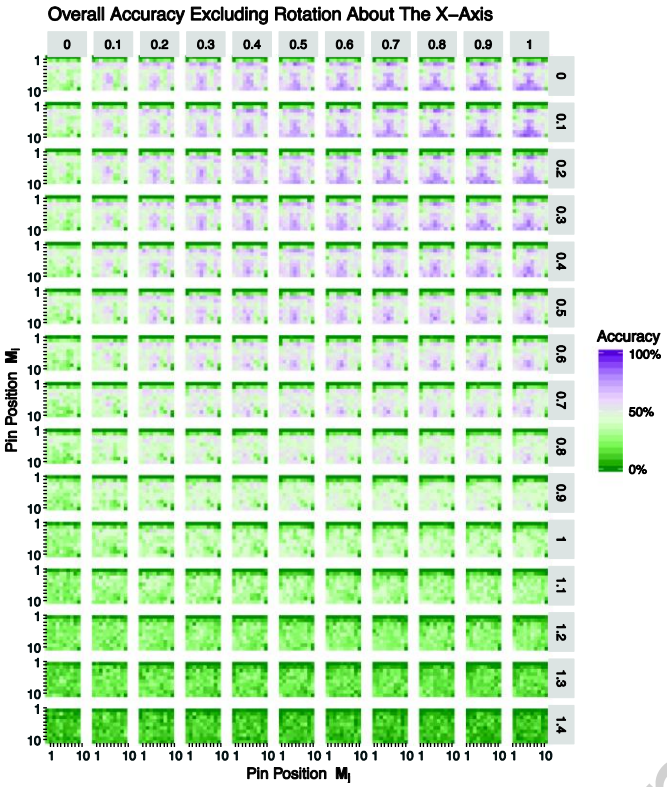

Figure 7: The overall accuracy for all permutations of the simulation excluding alpha rotations. Columns represent different values for friction; rows represent different values for elasticity and each square represents the accuracy at the initial position of the pelvis

(a) Normal sitting, the pelvis and femurs should be in a neutral position. The overlaid output of the algorithm shows the pelvis has rotated posteriorly and the femurs are positioned correctly distally. (b) Leaning Left, the pelvis should be orientated such that it is down on the left and the right femur abducted. The overlaid output shows that the pelvis is orientated correctly, the left femur is in the correct location however internally rotated, and the right femur is incorrectly orientated and positioned. (c) Obliquity, the pelvis should be orientated such that it is down on the left, the right femur should be extended, and the left femur flexed. The pelvis has rotated posteriorly but the orientation of the femurs is correct. (d) Obliquity, the pelvis should be orientated such that it is down on the left, the right femur should be extended, and the left femur flexed. The pelvis has rotated significantly posteriorly but the orientation of the femurs is correct.

Figure 8: Output of the algorithm for 4 of the 21 measurements included in this paper including a description of where the algorithm succeeded or failed.

4 Discussion

The low levels of accuracy for P_α; L_α; and R_α suggest that there is a limitation in the orientation prediction when considering these features. Upon visually inspecting the resting positions of these features in different simulations it is clear that the lack of force (muscles and upper body) keeping the pelvis upright is causing significant posterior pelvic tilt and then hence a high degree of extension in both the left and right hip. Additionally, the centre of mass for a seated person does not usually lie within the pelvic region of an individual. Repeating the experiment with the upper body being modelled to support the pelvis may improve the simulation results regarding rotation about the x axis as the pelvis will be supported by the spine interacting with the backrest.

The highest overall accuracy was obtained when the simulation parameters were $\mu_c = 1$, $e_c = 0$, and the starting location was $P_{(x,y,z)} = [0.02, 0.11, 0.3]$ metres which can be seen in Table 4. The highest overall classification accuracy is obtained when the starting location of the simulation is near the centre of the cushion which is where a clinician will attempt to seat a patient in the CBM mechanical shape sensor when capturing a measurement. From this set of input data it is suggested that the closer to the final resting position the simulation starts the greater the accuracy of classification will be. When excluding α-rotations from the results the accuracy improves to 92.8%. This was obtained when the simulation parameters were $\mu_c = 0.9$ and $e_c = 0$ and the starting location was $P_{(x,y,z)} = [-0.02, 0.11, 0.3]$ metres.

In all cases the best results for accuracy were obtained when $e_c \to 0$ and $\mu_c \to 1$. A high friction low elasticity cushion produced the best results in the simulation. An initial starting position of the pelvis of $P_x \cong 0$ and $-0.02 \leq P_y \leq 0.11$ produced the greatest accuracies for classification. These coordinates are near to the medial posterior of the seat which is where a clinician would attempt to seat a patient when taking a measurement or positioning someone for postural management.

The highest per feature accuracy was obtained when classifying pelvic rotation, however, in this dataset there were no non-neutral measurements for pelvic rotation. This is a limitation of this study. The dataset used to test the model in this instance was reliant on healthy volunteers who found it difficult to position their pelvis in such a way that a clinician would deem it non-neutral. This has highlighted a limitation of studies involving healthy volunteers for populations which contain individuals with musculoskeletal conditions. Whilst it is possible to state that the algorithm produces accurate classifications of the rotation about the y and z axis for healthy volunteers this should be tested on people with a wide range of musculoskeletal conditions.

The greatest benefit which this piece of work has highlighted is that we are able to improve how posture is visualised and communicated within clinics as demonstrated by the images in Figure 8. The simulation outputs the position and orientation of the pelvis and femurs. By decomposing the matrices for the orientation and positions it is possible to calculate the relative angles of the femurs to the pelvis. This would allow clinicians to easily compare the difference in two measured postures visually and numerically. A clinician measuring a posture that is the most amount of correction that could be applied safely at two different points in time could compare whether the amount of correction applied has changed. With additional work this technique will allow the measurement of seated postures at different moments and therefore will allow comparison of seated postures over time. As described in the introduction there does not exist a simple objective measure for seated

posture and techniques rely greatly on subjective measures and extensive clinical assessments. Further development of this algorithm will allow a snapshot of an individual's seated posture to be captured objectively.

This study used a 50th percentile male pelvis for the simulation. Whilst this is suitable in this instance as both participants are male it would not be suitable for the wider wheelchair user population. Future work should also take into account the musculoskeletal differences between sexes as the current 50th percentile male skeleton would not be representative of the majority of wheelchair users. Differences between sexes include a change in shape but also a change in the centre of gravity whilst sitting. Both of these factors are major contributors to the output of a physics based simulation.

5 Conclusion

This study has shown that it is possible to simulate a seated position using physics simulation and obtain a classification for the orientation of the pelvis and femurs about the y and z axes. The orientation of the pelvis and femurs about the x axis is influenced by the lack of an upper body and/or muscles and/or the position of the centre of mass of the whole system being located inside the pelvis causing it to rotate posteriorly.

The simulation should be further developed to more accurately model the seated position of an individual in a seated position as it could provide significant clinical benefits, such as comparison of body shape measurements over time.

The CBM can also be used to capture the unsupported shape of a patient. The unsupported shape of a patient is the recorded body shape when sat in the CBM with no external forces affecting the posture other than gravity and the surface the patient is seated on. This unsupported shape would reflect the patient's habitual posture; how the patient would sit without their posture correcting/supporting seat. From the unsupported surface shape certain anatomical landmarks can be identified using anthropometric feature extraction techniques facilitating the objective and unobtrusive measurement of and comparison of postures over time using the CBM and a DHM.

Capturing seated posture in this way; recording it objectively; and visualising it will allow clinicians to more easily compare the effects of interventions over time and measure improvements.

Acknowledgements

All co-authors testify that our article entitled 3D Posture Visualisation From Body Shape Measurements Using Physics Simulation, to Ascertain the Orientation of the Pelvis and Femurs in a Seated Position submitted to Computer Methods and Programs in Biomedicine has not been published in whole or in part elsewhere is not currently being considered for publication in another journal and all authors have been personally and actively involved in substantive work leading to the manuscript, and will hold themselves jointly and individually responsible for its content. The University of South Wales Institutional Review Board approved the study protocol and both participants who were members of the research team gave their informed consent prior to taking part in the study.

This work was supported by the Computing and Digital Economy Research Institute (Ref: 3127 R606), University of South Wales, Pontypridd, CF37 1DL, UK.

Conflict of interest

All co-authors declare no conflict of interests.

References

[1] R. Aissaoui, M. Lacoste, J. Dansereau, Analysis of sliding and pressure distribution during a repositioning of persons in a simulator chair, IEEE Transactions on Neural Systems and Rehabilitation Engineering 9 (2) (2001) 215-224. doi:10.1109/7333.928581.

[2] A. D. Goodworth, Y.-H. Wu, D. Felmlee, E. Dunklebarger, S. Saavedra, A Trunk Support System to Identify Posture Control Mechanisms in Populations Lacking Independent Sitting, IEEE Transactions on Neural Systems and Rehabilitation Engineering 25 (1) (2017) 22-30. doi:10.1109/TNSRE.2016.2541021.

[3] I. Cikajlo, Z. Matjacic, Directionally Specific Objective Postural Response Assessment Tool for Treatment Evaluation in Stroke Patients, IEEE Transactions on Neural Systems and Rehabilitation Engineering 17 (1) (2009) 91-100. doi:10.1109/TNSRE.2008.2010477.

[4] R. Palisano, P. Rosenbaum, S. Walter, D. Russell, E. Wood, B. Galuppi, Development and reliability of a system to classify gross motor function in children with cerebral palsy, Developmental Medicine & Child Neurology 39 (4) (2008) 214-223. doi:10.1111/j.1469-8749.1997.tb07414.x.

[5] C. Ryf, A. Weymann, The neutral zero method - A principle of measuring joint function, Injury 26 (1995) 1-11. doi:10.1016/0020-1383(95)90116-7.

[6] C. Ryf, A. Weymann, Range of motion-AO neutral-0 method: Measurement and documentation, Thieme Medical Publishers, New York, NY, USA, 1999.

[7] A. Partlow, A Knowledge Based Engineering System for the Prescription and Manufacture of Custom Contoured Seating for Clients with Severe Musculoskeletal and Postural Conditions, Ph.D. thesis, University of South Wales, Faculty of Computing, Engineering and Science, Pontypridd, Wales, UK (May 2014).

[8] A. Partlow, C. Gibson, J. Kulon, I. Wilson, S. Wilcox, Pelvis feature extraction and classification of Cardiff body match rig base measurements for input into a knowledge-based system, Journal of Medical Engineering & Technology 36 (8) (2012) 399-406. doi:10.3109/03091902.2012.712202.

[9] M. Voysey, J. Kulon, A. Partlow, C. Gibson, P. Rogers, A parametric human body modelling tool for the representation of sitting posture of individuals with profound musculoskeletal deformities, in: 2nd UK Patient Specific Modelling IPEM Conference, 2014, p. 106.

[10] S. Delorme, Y. Petit, J. de Guise, H. Labelle, C.-E. Aubin, J. Dansereau, Assessment of the 3-d reconstruction and high-resolution geometrical modeling of the human skeletal trunk from 2-d radiographic images, IEEE Transactions on Biomedical Engineering 50 (8) (2003) 989-998. doi:10.1109/TBME.2003.814525.

[11] M.-J. J. Wang, W.-Y. Wu, K.-C. Lin, S.-N. Yang, J.-M. Lu, Automated anthropometric data collection from three-dimensional digital human models, The International Journal of Advanced Manufacturing Technology 32 (1-2) (2007) 109-115. doi:10.1007/s00170-005-0307-3.

[12] A. Pfister, A. M. West, S. Bronner, J. A. Noah, Comparative Abilities of Microsoft Kinect and Vicon 3D Motion Capture for Gait Analysis, Journal of Medical Engineering & Technology 38 (5) (2014) 274-280. doi:10.3109/03091902.2014.909540.

[13] B. André, J. Dansereau, H. Labelle, Optimized vertical stereo base radiographic setup for the clinical three-dimensional reconstruction of the human spine, Journal of Biomechanics 27 (8) (1994) 1023-1035. doi:10.1016/0021-9290(94)90219-4.

[14] Y.-L. Lin, M.-J. J. Wang, Constructing 3D human model from front and side images, Expert Systems with Applications 39 (5) (2012) 5012-5018. doi:10.1016/j.eswa.2011.10.011.

[15] H. Labelle, J. Dansereau, C. Bellefleur, B. Poitras, C. H. Rivard, I. A. Stokes, J. de Guise, Comparison Between Preoperative and Postoperative Three-dimensional Reconstructions of Idiopathic Scoliosis with the Cotrel-Dubousset Procedure, Spine 20 (23) (1995) 2487-2492.

[16] J. Kulon, M. Voysey, A. Partlow, P. Rogers, C. Gibson, Development of a system for anatomical landmarks localization using ultrasonic signals, in: 2016 IEEE International Symposium on Medical Measurements and Applications (MeMeA), IEEE, Benevento, Italy, 2016, pp. 1-6. doi:10.1109/MeMeA.2016.7533764.

[17] S. J. Hillman, J. Hollington, A quantitative measurement method for comparison of seated postures, Medical Engineering & Physics 38 (5) (2016) 485-489. doi:10.1016/j.medengphy.2016.01.008.

[18] S. Haigh, J. Kulon, A. Partlow, P. Rogers, C. Gibson, A Robust Algorithm for Classification and Rejection of NLOS Signals in Narrowband Ultrasonic Localization Systems, IEEE Transactions on Instrumentation and Measurement (2018) 1-10. doi:10.1109/TIM.2018.2853878.

[19] J. Kulon, A. Partlow, C. Gibson, I. Wilson, S. Wilcox, Rule-based algorithm for the classification of sitting postures in the sagittal plane from the Cardiff Body Match measurement system, Journal of Medical Engineering & Technology 38 (1) (2014) 5-15. doi:10.3109/03091902.2013.844208.

[20] ROHO Inc., ROHO Quadtro Select High Profile Cushion (2016).

[21] E. Coumans, Bullet Physics Library (2015).

[22] Y. R. Serpa, M. A. F. Rodrigues, Parallelizing Broad Phase Collision Detection for Animation in Games: A Performance Comparison of CPU and GPU Algorithms, in: 2014 Brazilian Symposium on Computer Games and Digital Entertainment, Vol. 2014-Decem, IEEE, 2014, pp. 80-88. doi:10.1109/SBGAMES.2014.29.

[23] A. Visser, Z. Pan, S. van Duin, Bounding sphere CAD model simplification for efficient collision detection in offline programming, in: 2015 IEEE International Conference on Cyber Technology in Automation, Control, and Intelligent Systems (CYBER), IEEE, Shenyang, China, 2015, pp. 2029-2035. doi:10.1109/CYBER.2015.7288260.

[24] Blender Foundation, Home of the Blender project - Free and Open 3D Creation Software (2018).

[25] E. Coumans, Bullet 2.82 Physics SDK Manual, 2013.

[26] Zygote Media Group, Zygote::3D Male Skeleton (2015).

[27] K. Mamou, F. Ghorbel, A simple and efficient approach for 3D mesh approximate convex decomposition, in: 2009 16th IEEE International Conference on Image Processing (ICIP), IEEE, 2009, pp. 3501-3504. doi:10.1109/ICIP.2009.5414068.